Oscillatory settling in wormlike-micelle solutions: bursts and a long time scale

Nitin Kumar,[a] Sayantan Majumdar,[a] Aditya Sood,[b] Rama Govindarajan,[c] Sriram Ramaswamy [a] and A.K. Sood[a]

Received 11th January 2012, Accepted 14th February 2012
Published in Soft Matter
DOI: 10.1039/c2sm25077b

We study the dynamics of a spherical steel ball falling freely through a solution of entangled wormlike micelles. If the sphere diameter is larger than a threshold value, the settling velocity shows repeated short oscillatory bursts separated by long periods of relative quiescence. We propose a model incorporating the interplay of settling-induced flow, viscoelastic stress and, as in [PRE 66, 025202(R) (2002) and PRE 73, 041508 (2006)], a slow structural variable for which our experiments offer independent evidence.

A sphere falling through a Newtonian fluid at low Reynolds number Re [1] reaches a steady terminal velocity through the interplay of gravity, buoyancy and viscous drag. This simple system, and its extensions to unsteady high Re flow, are well understood and form the basis of falling ball viscometers [2]. In non-Newtonian fluids unsteady settling is observed [3,4] even at low Re. Mollinger *et al.* [3] observed periodic stick-slip settling in the beginning of the fall and investigated the effect of wall confinement on the baseline settling velocity and the frequency of unsteady events. Jayaraman *et al.* [4] found a transition from steady to *irregular unsteady* settling, remarked that the relevant control parameter was the shear rate, $\dot{\gamma} = v_b/d$ (v_b & d being the baseline velocity and sphere diameter respectively), and emphasized the importance of the negative wake behind the particle [5,6]. It was suggested [4] that the oscillations were a result of the formation and breakup of flow-induced structures, known to arise in concentrated micellar systems [7–9].

In this paper we investigate the sedimentation of spherical metallic particles through an entangled wormlike-micelle solution [9] of the surfactant CTAT (Cetyl Trimethyl Ammomium p-Toluenesulphonate) in brine. We report here for the first time that spheres larger than a critical size not only undergo unsteady motion, but also show sustained, repeated bursts of oscillations superposed on a constant baseline velocity as shown in Fig. 1. The intra-burst oscillation period $\tau_{fast} \sim d/v_b$; the time between bursts τ_{slow} is at least an order of magnitude larger. We account for these results through a model incorporating shear-induced coupled oscillations of viscoelastic stress components and a slow structural relaxation [10,11] giving rise to τ_{slow}. We suggest that equilibrium fluctuations, i.e., without imposed flow, should show signatures of the structural variable.

Experiments were conducted on two different samples, Gel A comprising 2 wt% CTAT + 100 mM NaCl and Gel B with 2.2 wt% CTAT + 82 mM NaCl. Rheological measurements were carried out on a Paar Physica MCR 300 Rheometer in the cone-plate geometry. The frequency sweep and flow curve of Gel A give an extrapolated zero-shear-rate viscosity of 17.8 Pa s at 25°C, onset of shear thinning at a shear rate $\dot{\gamma}_c \sim 0.4 s^{-1}$. The linear viscoelasticity is Maxwellian with a relaxation time $\omega_{co}^{-1} \simeq 1.34$ s. The corresponding numbers for Gel B are 8.5 Pa s, 1.5 s^{-1} and 0.97 s respectively. These systems are in the parameter range where shear banding instabilities and spatiotemporal rheochaos are expected above a critical shear rate [12–15].

A transparent cylindrical tube of diameter $D = 5.4$ cm and height 40 cm was filled with the wormlike-micelle solution. Steel balls of diameters d from 3 mm to 8 mm were introduced one at a time into the solution with zero initial velocity using an electromagnet positioned accurately to ensure that the balls sediment along the axis of the tube. Images of the falling balls were recorded using a Citius C100 Centurio camera capable of capturing 423 frames per second at its full resolution of 1280×1024 pixels. Image analysis was done on the captured frames to extract information about the position and velocity of the ball as a function of time. Experimental runs were separated by at least 30 minutes in order to ensure complete relaxation and homogenization of the fluid prior to each run.

We present first our results for Gel A. Fig. 1 shows velocity-time plots of various diameters d. For $d = 0.4cm$ (Fig. 1(a)) the ball quickly achieves a steady terminal velocity as ex-

[a] *Department of Physics, Indian Institute of Science, Bangalore 560 012, India*
[b] *Department of Materials Science and Engineering, Stanford University Stanford, CA 94305*
[c] *Engineering Mechanics Unit, Jawaharlal Nehru Centre for Advanced Scientific Research, Bangalore 560 064, India.*

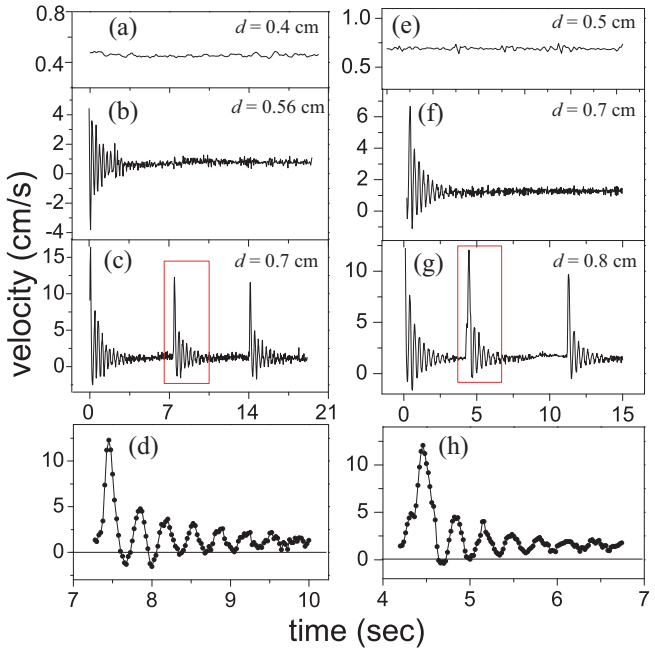

Fig. 1 Velocity as a function of time: For Gel A; (a) d=0.4 cm, (b) d=0.56 cm and (c) d=0.7 cm. In (d), the velocity variation marked in (c) has been expanded. For Gel B: (e) d=0.5 cm, (f) d=0.7 cm and (g) d=0.8 cm. In (h), the velocity variation marked in (g) has been expanded.

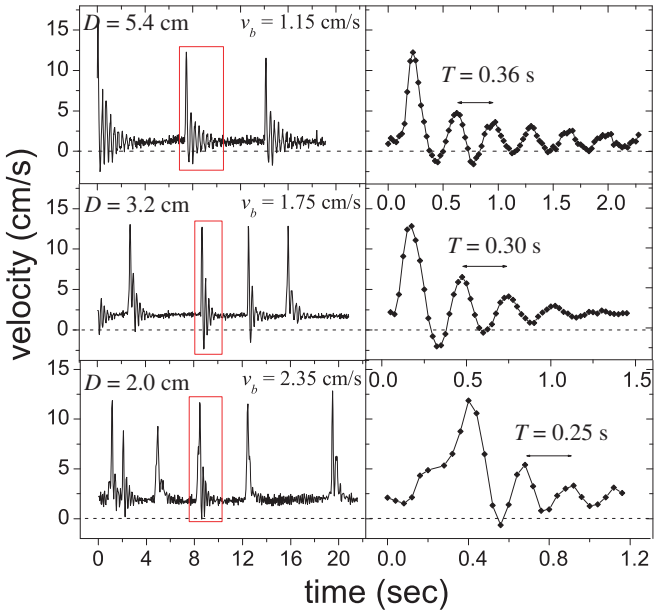

Fig. 2 The motion of 0.7 cm ball in CTAT (2wt%)+100 mM NaCl dropped in tubes of various diameters. Note the increase in the baseline velocity, v_b in thinner tubes (diameter D) followed by decreasing time-period (T) of burst oscillations.

pected in the Stokesian limit for a Newtonian fluid. For $d = 0.56cm$ (Fig. 1(b)) a strong oscillatory transient as in noted by King and Waters[16] is seen before terminal velocity sets in. For $d = 0.70cm$ (Fig. 1(c)), oscillations are seen to occur in repeated bursts on top of a constant baseline velocity v_b, and are sustained throughout the fall of the particle. The time between bursts is 4 to 7 sec, at least an order of magnitude larger than the oscillation period ~ 0.3 s within the burst. Fig. 1(d) is an enlarged version of the bursts highlighted in Fig. 1(c). Within each burst the oscillations have an exponentially damped sinusoidal form; the total number of such bursts before the ball reaches the bottom is too small for us to conclude whether their timing is truly periodic or merely distributed narrowly about a well-defined mean. The figures also show that the oscillations are occasionally large enough to result in a small negative velocity; i.e., the ball sometimes jumps up against gravity. Visual observation shows a strong negative wake behind the ball during the burst. Gel B shows similar behaviour as seen in Figs. 1(e-h). Interestingly, it should be noted that the baseline velocities scale as d^2, consistent with Stokes's Law. Jayaraman *et al.*[4] remarked that oscillations set in at velocity gradients v_b/d close to the frequency where G'' (loss modulus) begins to increase. We do not observe such a correspondence.

Fig. 2 shows the effect of wall confinement for a ball of diameter d=0.7 cm. A comparison of baseline velocities v_b in tubes of diameter D = 5.4 cm, 3.2 cm and 2.0 cm shows that v_b increases as D decreases, an effect opposite to that known in Newtonian fluids[2]. The effect is observed for smaller diameters as well. We find that within a burst the time-period T (as marked in Fig. 2) decreases with decreasing D. Local thinning caused by flow alignment of micellar structure along the walls, expected to be more pronounced in narrower tubes, is a likely explanation for these observations.

In order to account for the observation of bursts and oscillations, we now offer a simple theoretical model based on the interplay of the orientation field of the micelles and flow generated by the settling particle. We emphasize that our intent is to offer a rational account of the observed phenomena, not to reproduce them in full detail. Further, we will show that the model, although schematic in nature, nonetheless leads to other predictions that can be tested in independent experiments. We start by summarizing some features of the behaviour shown in Fig. 1(c). The phenomenon of primary interest is the observation of rapidly oscillatory bursts repeated at fairly regular long intervals. Each burst is damped in a roughly exponential manner, with a time constant noticeably smaller than the interval between bursts, i.e., each successive burst emerges from a flow that has become nearly quiescent. The baseline settling speed $v_0 \simeq 1.15$ cm/s, with oscillations up to 12 cm/s. The resulting shear-rate at the scale of a particle (diameter $d \simeq 0.7$ cm) is $\dot{\gamma} = v_0/d \simeq 1.64$ to 17.1 s^{-1},

corresponding to a timescale $\dot{\gamma}^{-1} \simeq .06$ s to 0.6 s for the accumulation of a strain of unity. The micellar solution has a measured zero-shear-rate viscosity of $\eta_0 \simeq 18.0$ Pa s, thinning under shear to about 1.4 Pa s, and a viscoelastic or orientational relaxation time $\tau_v \simeq 1.34$ s. The Reynolds number at the particle scale is thus at most 6×10^{-4}. The settling particles are steel (density $\rho \simeq 8$ g/cm^3) and hence would reach terminal velocity, if the viscosity were constant, in a time of order $\tau_i = \rho d^2/18\eta_0 \simeq 1.2$ to 15.6 millisec depending on whether one takes the zero-shear or thinned value for the viscosity. The observed period *within* the bursts is $T_1 \simeq 0.36$ s, and the period *between* bursts is $T_2 \simeq 9$ s. T_1 and τ_v are comparable to $\dot{\gamma}^{-1}$, $T_2 \gg T_1, \tau_v$, and τ_i is much smaller than all of these. Both acceleration and advection can thus be neglected in the Navier-Stokes equation, and we can work in the limit of Stokesian hydrodynamics, keeping track of stresses arising from the complex nature of the micellar solution. We now present our model for the coupled dynamics of the particle and the micellar medium.

Consider a particle settling under gravity in a wormlike-micelle solution with velocity field $\mathbf{u}(\mathbf{r})$ at location $\mathbf{r}$, with solvent viscosity η and a contribution $\sigma^{(m)}$ to the stress tensor from the conformations of the micelles. The steady Stokes equation

$$-\eta\nabla^2\mathbf{u} = -\nabla P + \mathbf{W} - \nabla\cdot\sigma^{(m)} \tag{1}$$

balances viscous, pressure, and conformational stresses against the gravitational force from the buoyant weight $\mathbf{W}$ of the particle. Inverting (1) and choosing the particle's centre of mass as origin, the settling velocity

$$\mathbf{v} = \mathbf{v}_0 + \int d^3r\, \mathbf{H}(\mathbf{r})\cdot\nabla\cdot\sigma^{(m)}(\mathbf{r}) \tag{2}$$

where $\mathbf{H}$ is the incompressible Stokesian hydrodynamic propagator and $\mathbf{v}_0$ is the Stokes settling velocity in the absence of contributions from micelle conformations, and the second term on the right in (2) contains modifications of the settling speed due to micellar stresses around the particle. The dynamics of $\sigma^{(m)}$

$$\frac{D\sigma^{(m)}}{Dt} = \lambda_0\mathbf{A} + \lambda_1[\mathbf{A}\cdot\sigma^{(m)}]_{ST} - \frac{1}{\tau}\sigma^{(m)} \tag{3}$$

combines flow-orientation coupling and relaxation, familiar from a variety of contexts including general rheological models, rheochaos, and nematic hydrodynamics[11,17–19]. Here D/Dt is a time derivative comoving and corotating with the fluid, $\mathbf{A}$ is the symmetric deformation-rate tensor, and the subscript ST denotes symmetric traceless part.

It is useful to work with a simple model extracted from (2) and (3). From (2) we suggest that a component p of the micellar stress, presumably originating in micelle orientation around the particle alters the settling speed: $v = v_0 + p$ where v_0 is the speed in the absence of contributions from the micellar stress. The form of (3) suggests the schematic dynamics $\dot{p} \sim v + vp + vq - p + ...$, where production by shear competes with relaxation to local equilibrium. As in the Johnson-Segalman model[17] or nematic hydrodynamics[18–21] shear, through v, naturally couples p to other components q, which in turn have a similar dynamics. The ellipsis indicates terms of higher order in p and q, and we have assumed that the local shear-rate is proportional to the settling speed v. The structure of these equations raises the possibility of oscillations with a timescale set by the shear-rate. Such shear-induced mixing of micellar stress components is very likely the mechanism for the oscillations *within* a burst, as their frequency, as seen from the numbers reported above, lies right in the middle of the range of particle-scale shear-rates $\dot{\gamma}$. The timescale associated with the repeated appearance of the bursts is far longer, as remarked above, and must arise from a distinct process. We propose that it enters through the memory mechanism introduced by Cates and coworkers[10,11] that we incorporate and explain in detail below. Assembling these ingredients we replace the dynamics of the micellar stress tensor (3) by the effective model

$$\dot{p} = \lambda_0 v + \lambda_1 vp + \lambda_2 vq - \zeta p - sw - \mathcal{P}(p,q), \tag{4}$$

$$\dot{q} = \mu_0 v + \mu_1 vp + \mu_2 vq - \gamma q - \mathcal{Q}(p,q), \tag{5}$$

and (2) by the schematic relation $v = v_0 + p$ already mentioned above. The terms $\mathcal{P}$ and $\mathcal{Q}$ in (4), (5) incorporate nonlinearities that would arise naturally in a local thermodynamic approach[18,20] where p and q are related to the orientational order parameter. The coefficients λ_i, μ_i are flow-orientation couplings, corresponding to similar terms in (3) and best understood from nematic hydrodynamics[18–23] . We have allowed the relaxation of p to occur through two channels: locally in time via the term ζp in (4), and through the intervention of a structural variable*[10,11,24]

$$w(t) = \int_{-\infty}^{t} dt' e^{(t-t')\Gamma} p(t') \tag{6}$$

determined by the past history of p. Equivalently,

$$\dot{w} = \Gamma(p - w), \tag{7}$$

whence it is clear that w becomes identical to p only for $\Gamma \to \infty$. We see formally that w and p stand in the same relation as position and momentum for an oscillator, even in regard to the relative signs of the coefficients of w in (4) and p in (7). We emphasize that this relation has nothing to do with real inertia: our equations are meant to describe the viscosity-dominated regime. Equation (7) says, plausibly, that

* In principle q could also relax through such a memory mechanism. For simplicity we have not explored this possibility.

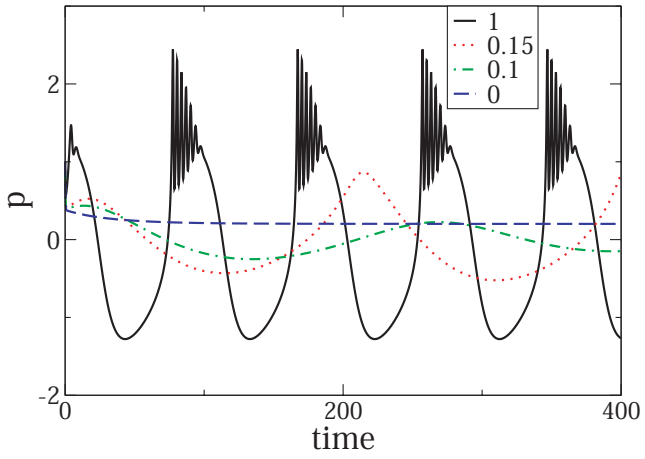

Fig. 3 Oscillations in the settling speed from (4), (5), (7) for several α as indicated. Note the two distinct timescales, within and between bursts.

an imposed nonzero local alignment p shifts the equilibrium value of an underlying structural quantity such as the Maxwell viscoelastic time of the material [10,11] or the micelle length [24]. As in those works, we assume that the parameters Γ and s of this mechanochemical coupling are properties of the unsheared system; our observations are consistent with $\Gamma \ll \dot{\gamma}$, the particle-scale shear rate.

The parameter space of (4), (5) and (7) is vast, and our limited exploration finds regimes of spontaneous oscillation. Fig. 3 shows p (which is v apart from a constant) as a function of time for the model equations $\dot{p} = A_1 - A_2 p - A_3 q - A_4 w + A_5 p^2 - A_6 p^3$, $\dot{q} = \alpha(B_1 - B_2 p - q + B_3 p^2)$, $\dot{w} = \Gamma(p - w)$†, bringing in q gradually by stepping $\alpha = 0, 0.1, 0.15 \& 1.0$.

Our model, constructed using physically plausible arguments, reproduces key features of the experimental observation, namely, a rapid oscillation timescale clearly associated with the shear and a much slower oscillation of distinct origin. Further, if the contribution of q is diminished by reducing α only the slow oscillation of p against w is seen. Only when α is large are the rapid oscillations seen, and these disappear on a timescale much smaller than that associated with the slow oscillation.

As noted in [11,25], equations of the general form (4) - (7) are widespread in the neuronal modelling literature [26,27]. Among the most robust features of such models are oscillations with a bursty character, and the coexistence of two or more widely separated timescales. In the neurophysics literature the introduction of an additional slow "recovery variable" was motivated in part by detailed knowledge of the electrophysiology of the axon [27]. The success of our model in capturing essential features of our experiment encourages us to suggest independent experimental tests for the coupled dynamics of micellar stress p and "structure" w in the absence of shear. If not for the structural variable w we should have a conventional Johnson-Segalman or nematogenic fluid *at rest*, whose dynamical response and spontaneous fluctuations are overdamped. However, in (4) and (7) the micellar stress p and the structural variable w act like the momentum and coordinate of an oscillator. And precisely because we require w to be *slow*, the damping coefficient $\Gamma \ll s$, the coupled dynamics is in the *underdamped* regime, so their linear response to disturbance must be oscillatory. Further, if we augment the dynamical equations (4), (7) with thermal noise, the resulting Fourier-transformed dynamic correlation functions of the system in the absence of the falling ball should show a peak at a frequency around that of the *slow* oscillation seen in the falling-ball experiments.This feature seems to be quite robust, relying only on the assumption that the parameters in the dynamical equation for the structural variable w depend negligibly on the shear rate. This property is shared by the models presented by Cates *et al.* [10,11] and emerges naturally from microscopic kinetic models [9]. However, it is conceivable that the kinetics in our system is such that w becomes slow only under strong imposed shear, in which case the *equilibrium*, i.e., unsheared, fluctuations of the coupled $p - w$ dynamics would be overdamped. A search for such oscillatory response or correlation in *equilibrium* experiments would help resolve this issue. This in turn requires a dynamical probe of local anisotropy; a possible scheme might be to suspend droplets of a strongly flow-birefringent fluid in the wormlike-micelle solution, and measure the power spectral density of the spontaneous fluctuations in the light intensity seen through crossed polars.

We emphasize that our simple model aims primarily to capture the bursts and the two disparate time-scales in the problem. Within the limitations of this approach, we have suggested possible independent tests of the model. Further experiments with different viscoelastic parameters and particle shapes should lead us to a more quantitative theory, at the level of reduced models like (4) - (7) or a more complete hydrodynamic treatment. A better understanding, perhaps in terms of micelle kinetics [9], of the slow structural variable in our system is of particular importance.

To summarise: we have isolated the mechanism for the observed oscillatory descent of a sphere through a wormlike-micelle solution. The oscillations produced by (4)-(7) show two broadly different timescales, as in the experiments, although the detailed form of the oscillations is not identical to those observed. One timescale is associated with the shear, the other with the coupled dynamics of micellar stress and a structural parameter such as micellar length or equilibrium Maxwell time. We argue that this second timescale is likely to appear in the unsheared system in independent measurements

† with parameter values A_1=3, A_2=10, A_3=1, A_4=A_5=6, A_6=1, B_1=3, B_2=12, B_3=6 & Γ=0.006

of the autocorrelation of spontaneous fluctuations of stress or orientation, and suggest experiments to test this possibility.

Flow-birefringence studies[28,29] focusing on the velocity and orientation fields of the medium around the falling ball will offer further insight into the detailed mechanism underlying the phenomena presented in this work. We note that the birefringence contrast as seen by Rehage *et al.*[28] in studies on solutions similar to ours, is small. Such measurements on our system will therefore require a careful high resolution study, which we defer to later work.

Numerical studies of the complete hydrodynamic equations for orientable fluids, studying the effect of the gravitational settling of a sphere through the medium, should see these curious oscillations, and will allow us to converge on the correct effective model of the general type of (4) - (7).

We thank M.E. Cates for useful discussions. NK and SM are grateful to the University Grants Commission, India for support. AKS and SR respectively acknowledge a CSIR Bhatnagar fellowship and a DST J.C. Bose fellowship.

References

1 G.G. Stokes, Trans. Cambridge Philos. Soc. **9**, 8 (1851).

2 R.P. Chhabra, *Bubbles, Drops and Particles in non-Newtonian fuids*, (CRC Press, Boca Raton FL, 1992).

3 A.M. Mollinger, E.C. Cornelissen, B.H.A.A. van den Brule, J. Non-Newtonian Fluid Mech. **86** (1999) 389-393.

4 A. Jayaraman and A. Belmonte, Phys. Rev. E **67**, 065301(R) (2003).

5 O. G. Harlen, J. Non-Newtonian Fluid Mech. **108** (2002) 411-430.

6 C. Bisgaard and O. Hassager, Rheol. Acta **21**, 537 - 539 (1982).

7 L.M. Walker, Curr. Opin. Colloid Interface Sci. **6**, 451 (2001).

8 H. Rehage and H. Hoffmann, Faraday Discuss. Chem. Soc. **76**, 363 (1983).

9 M.E. Cates and S.M. Fielding, Adv. Phys. **55**, 799 (2006).

10 M.E. Cates, D.A. Head and A. Ajdari, Phys. Rev. E **66**, 025202(R) (2002)

11 A. Aradian and M. E. Cates, Phys. Rev. E **73**, 041508 (2006).

12 R. Bandyopadhyay, G.Basappa and A. K. Sood, Phys. Rev. Lett. **84**, 2022-2025 (2000).

13 R. Ganapathy and A. K. Sood, Phys. Rev. Lett. **96**, 108301 (2006).

14 R. Ganapathy, S. Majumdar and A. K. Sood Phys. Rev. E **78**, 021504 (2008).

15 R. Ganapathy and A. K. Sood, J. Non-Newtonian Fluid Mech. **149**, 78 (2008).

16 M. J. King and N. D. Waters, J. Phys. D: Appl. Phys., **5**, 141, (1972).

17 M. D. Johnson and D. Segalman, J. Non-Newtonian Fluid Mech. **2**, 255 (1977)

18 M. Das, B. Chakrabarti , C. Dasgupta, S. Ramaswamy, and A. K. Sood, Phys. Rev. E **71**, 021707 (2005).

19 G. Rienäcker, M. Kröger, and S. Hess, Phys. Rev. E **66**, 040702R (2002); Physica A **315**, 537 (2002).

20 P. G. de Gennes and J. Prost, *The Physics of Liquid Crystals* (Clarendon Press, Oxford, 1995).

21 D. Forster Phys. Rev. Lett. **32**, 1161 (1974).

22 H. Stark and T. C. Lubensky, Phys. Rev. E **67**, 061709 (2003).

23 In the underlying hydrodynamic equations there are only two independent couplings of this form, which enter both in the equation for $\sigma^{(m)}$ and in the generalized Stokes equation for the velocity. Equations (4) - (7) have been written in a form in which the coefficients in the Stokes equation have been absorbed into a rescaling of the orientation variables. We have allowed for distinct values for the flow-orientation couplings for p and q to take into account the possibility of detailed differences in orientation and flow fields at various locations around the particle.

24 S. M. Fielding and P. D. Olmsted, Phys. Rev. Lett. **92**, 084502 (2004).

25 L. Giomi, L. Mahadevan, B. Chakraborty, and M.F. Hagan, Phys. Rev. Lett. **106**, 218101 (2011)

26 See, e.g., J. D. Murray, Mathematical Biology: I. An Introduction (Springer, New York, 2007); the mathematical link between complex-fluid rheology and neuronal modelling has been discussed in[11] and, in an active-matter context, by L. Giomi *et al.*, Phys. Rev. Lett. **106**, 218101 (2011)

27 J. L. Hindmarsh and R. M. Rose, Proc. R. Soc. Lond. B **221**, 87-102 (1984)

28 H. Rehage, H. Hoffmann, and I. Wunderlich, Ber. Bunsenges. Phys. Chem. **90**, 1071 - 1075 (1986).

29 K. Nijenhuis *et al.*, in Springer Handbook of Experimental Fluid Mechanics, C. Tropea, A.L. Yarin and J.F. Foss (eds.), Springer-Verlag, Berlin (2007)